High Impedance Fault Detection in Real-Time and Evaluation Using Hardware-In-Loop Testing

Bhandia, Rishabh; Chavez, Jose J.; Cvetković, Miloš; Palensky, Peter

DOI
10.1109/IECON.2018.8591824

Publication date
2018

Document Version
Accepted author manuscript

Published in
Proceedings IECON 2018 - 44th Annual Conference of the IEEE Industrial Electronics Society

High Impedance Fault Detection in Real-Time and Evaluation using Hardware-in-Loop Testing

Rishabh Bhandia
Deprtment of Electrical Sustainable Energy
Delft University of Technology
Delft, The Netherlands
R.Bhandia@tudelft.nl

Jose J. Chavez
Deprtment of Electrical Sustainable Energy
Delft University of Technology
Delft, The Netherlands
J.J.ChavezMuro@tudelft.nl

Miloš Cvetković
Deprtment of Electrical Sustainable Energy
Delft University of Technology
Delft, The Netherlands
M.Cvetkovic@tudelft.nl

Peter Palensky
Deprtment of Electrical Sustainable Energy
Delft University of Technology
Delft, The Netherlands
P.Palensky@tudelft.nl

***Abstract*—High Impedance Fault (HIF) is a low fault current event which cannot always be efficiently detected or cleared by conventional protection systems. Voltage or current signal distortions are often a possible indicator of HIF signatures which need to be carefully analyzed. This paper proposes a new technique based on second-difference approach to detect signal distortions. The technique does not require large database and is computationally very lightweight. The performance of the proposed technique is compared against commercial protection relays connected in Hardware-in-Loop (HIL) mode to a Real Time Digital Simulator (RTDS) simulating HIF in a IEEE 9-bus system. Test result evaluation show that the proposed technique is accurate and dependable.**

***Keywords*—High Impedance Fault, Power system protection, Waveform analytics, Distortion detection, Power system reliability.**

I. INTRODUCTION

High Impedance Faults (HIFs) are a unique problem for the conventional protection systems. They produce very low fault current which is not enough to trip the existing protection devices. A HIF occurs mostly when a primary conductor makes an unwanted contact with a tree or road or any object restricting the flow of fault current [1]. The Line Protection Sub-Committee of the Power Systems Relaying Committee has prepared a report on High Impedance Fault detection technology which states that the success rate of conventional protection systems against HIF is only 20% [1-2]. An undetected HIF will lead to downed conductors and arcing which can also be very hazardous to public safety.

Research has been going on to address the issue of HIF from 1970s. Mathematical morphology technique has been used in [2] and mathematical morphology along with magnetic field signature analysis has been used in [3]. In [4-6] one can find exhaustive analysis of all the techniques proposed till now to detect HIF. In [7] neural network is combined with time-frequency transformation to detect HIF, while [8-9] use adaptive neural network schemes to detect HIF. Wavelet transforms have been used in [10], whereas Kalman filter has being used in [11-12] to detect HIF.

Majority of the techniques discussed before have contributed a lot to the understanding of HIF related phenomenon and methods to detect it. However some of the techniques discussed are time–consuming while some require considerable computational power. Some techniques would have to be implemented in standalone devices/ equipment which will lead to more costs and increase the complexity of grid infrastructure. In this paper, a very simple yet robust technique to detect HIF based on the mathematical concept of second-order difference is proposed. Existing protection systems are already very efficient in detecting the low-impedance faults (LIF). The algorithm we propose can implement/embed the HIF detection technique code in the current protection relays easily, which means complete HIF and LIF protection at negligible additional cost.

The report in [1] states that the HIF studies have primarily focussed on finding some characteristics in the current and voltage waveform that would make the detection of HIF practical. In this paper we use an HIF detection technique based on waveform analytics. The technique has been implemented in [13] with positive results. In this paper we modify the technique by adding a low pass filter to filter out harmonics and investigate its performance vis-à-vis existing commercial protection relays. This detection technique employs second-difference mathematical approach to detect HIF. The detection technique leverages the sinusoid nature of voltage and current waveforms in the AC grid as explained in the subsequent sections. The waveforms are generally pure sinusoids in nature unless there are distortions due to fault or fault like conditions. LIF are easy to detect as compared to HIF, which causes few distortions and current and voltage levels do not change significantly. The distortion detection technique aims to detect these small distortions in the waveforms to classify whether it is a harmful event for the stable operations of the grid. A similar difference based approach has also been used for current transformer saturation and detection in [14].

In this paper, a Hardware-in-Loop (HIL) test connecting a protection relay to a Real Time Digital Simulator (RTDS) was conducted in order to show the performance of actual commercial protective relays under HIF. IEEE 9-bus test system with a HIF was developed in the RSCAD platform. At the same time we import the simulation data from RTDS to MATLAB where we implement the distortion detection technique. We conduct simulations in RTDS to create a real

time environment and add more credibility to the results. Two different protection functions are set in the relays and the detection results are compared against the results obtained from the distortion detection technique.

The paper has been structured as following: Section II discusses the standard models used for testing. Section III describes the distortion detection technique in detail. Section IV presents and discusses the simulation and HIL testing results. Finally, Section V presents the conclusions.

II. Distortion Detection Technique

This section has been divided in two parts. The first subsection explains the distortion detection technique and the second subsection explains how the technique is implemented as seen in [13].

A. Distortion Detection Technique as Difference Function

The current and voltage waveforms in an AC power system are sinusoid and can be described as complex exponentials using Euler formula as seen in (1)

$$e^{j\omega t} = \cos\omega t + j\sin\omega t \qquad (1)$$

where ω is the angular frequency (*in radians per second*), t is time (*seconds*) and j is the imaginary unit.

The distinct characteristic of an exponential function is, the rate of increase or decrease of an exponential function is proportional to the value of the function at that instant. An additional characteristic of a complex exponential function is that it is not infinitely increasing or decreasing. These characteristics of the complex exponential functions are used for devising the difference based distortion detection technique. The distortion detection technique proposed in this paper uses the first difference instead of continuous differentials since the signals that are being processed are sampled voltages and current in the power grid. Mathematical formulation of the previously illustrated concept is presented next.

The sampled signal $f[k]$, as shown in Fig. 1 is a general representation of any voltage or current signal measured from the grid. Assuming the signal as a sine wave of period T, which can be sampled at N samples per cycle, the samples could be denoted as: $n...k, k+1, k+2...n+N$. The samples are equally spaced in time-domain at an interval of length h, such that:

$$T = h \bullet N \qquad (2)$$

Let $g[k]$ be the difference of the sample values at sample k and $k+1$, the first difference at k can be written as:

$$g[k] = \frac{f[k] - f[k-1]}{h} \qquad (3)$$

Similarly at $k+1$:

$$g[k+1] = \frac{f[k+1] - f[k]}{h} \qquad (4)$$

Now, for a pure sine wave, using (3) and (4), it can be written that:

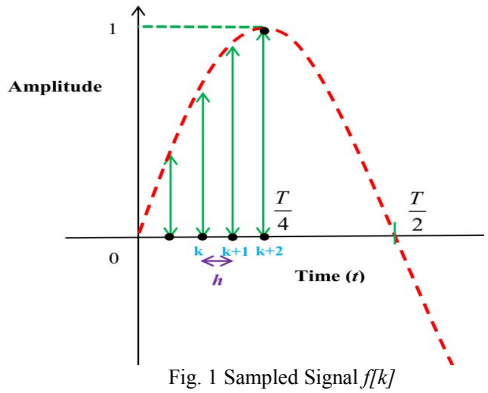

Fig. 1 Sampled Signal *f[k]*

$$g[k] > g[k+1], k \in \{n, n+\frac{T}{4}\} \cup \{n+\frac{T}{2}, n+\frac{3T}{4}\} \qquad (5)$$

$$g[k] < g[k+1], k \in \{n+\frac{T}{4}, n+\frac{T}{2}\} \cup \{n+\frac{3T}{4}, n+T\} \qquad (6)$$

Hence if $f[k]$ is a pure sine wave, (5) and (6) will always hold true. In case, (5) or (6) are violated, the violation will be recorded as a distortion. The violation will be interpreted as a distortion as for that instant, $f[k]$, would cease to be a pure sine wave.

B. Distortion Detection Technique Implementation

In this subsection, we discuss the detection technique implementation in detail. The schematics of the procedure can be seen in Fig. 5. The electrical current and voltage waveform measurements are taken from the grid and analysed in steps as described below:

1) Low-Pass Filter

The firsts step is passing the waveforms through a low pass filter with the cut-off frequency being the fundamental frequency. This filter performs satisfactorily the frequency rejection above the first harmonic in order to avoid false flags by the technique when a HIF is not happening in the system.

2) Distortion Detection

The mathematics governing the Distortion Detection technique has been explained in the previous section. The main objective of this block is to implement the distortion detection technique. The input to this block is current or voltage waveform $f[k]$, measured with a sampling rate R from a particular node in the grid. Whenever this block detects violation of (5) or (6), a flag is raised and distortion reported. The output of this block is (d,t) where d indicates the occurrence of the distortion at time t. We can define d as, $d=1$, if distortion is detected and $d=0$, if distortion is not detected. The output of this block serves as an input to the Distortion Recorder block.

3) Distortion Recorder

The objective of this block is to store the distortion occurrence data from Distortion Detection block in a data

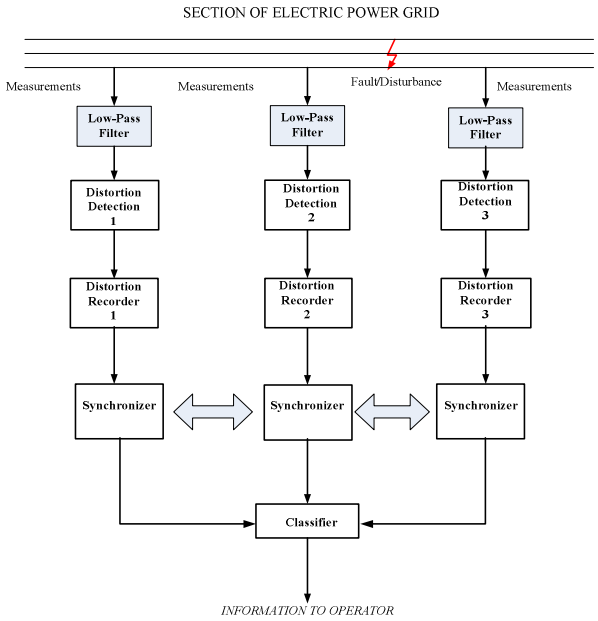

Fig. 2. Distortion Detection Technique Implementation flowchart

set of a specified length as explained below. This data set is called Memory Buffer. The input to this block is (d,t). The input data is collected and processed by an N sample window as it moves along the entire waveform. The size of the window is user-dependent and could vary from one measuring device to another. If we have m measuring devices such that $i = 1,2,3...m$, then the memory buffer W_i in the time interval of (a_i, b_i) can be represented as:

$$W_i = \{(d_f, t_f) \mid d_f \in \{0,1\}, t_f \in (a_i, b_i), f = (1,2,3...N)\} \quad (7)$$

The memory buffer W_i contains the instants of occurrence and non-occurrence of distortions in a fixed length of time interval (a_i, b_i). Eq. (7) is the output from the distortion recorder block and serves as an input to the synchronizer block.

4) Synchronizer

The synchronizer block helps in aligning all the reported distortions such that a correct classification can be achieved. The occurrence of a disturbance at a certain point in the grid will not have the same impact over the entire section of the grid. For the same distortion, some measurement devices may report numerous and frequent distortion levels, some lower and some may not report any distortion at all. Also, the measurement devices may not have uniform sampling rates.

One of the pre-requisites for accurate analysis is that all the data collected should be synchronized. If not, it will cause false flag error leading to wrong results. Hence, for synchronization, comparison and further analysis of the distortion detection data we need a window of fixed time interval to collect all reporting's from different measurement devices during that time interval. The device with the highest sampling rate will report maximum distortion detection data in that fixed time interval compared to other measurement devices. The design of the smallest time interval for a single data recording of the window should be small enough to record reporting's from the measurement device of the highest sampling rate. Hence, the measurement device with the highest sampling rate forms the base reference for other measurement devices with lower sampling rates and consequently lower reporting rate of the distortion data. Henceforth, the design of the base window is governed by the measurement device of the highest sampling rate. The base window A can be represented as:

$$A = (a_{base}, b_{base}) = \bigcap_{i=1}^{n} (a_i, b_i) \quad (8)$$

The curtailed memory buffer, $\widetilde{W}_i$, within the size limits of the base window can be represented as:

$$\widetilde{W}_i = \{w_i = (d_f, t_f) \mid w_i \in W_i \text{ and } t_f \in (a_{base}, b_{base}) \text{ and } d_f \in \{0,1\}\} \quad (9)$$

The last processing step of this block is to sum the values of the distortion occurrences d_f in $\widetilde{W}_i$. We can write:

$$C_i = \sum_{p=1}^{|\widetilde{W}_i|} d_p \quad (10)$$

Thus, (10) is the output from each synchronizer block sent to the classifier.

5) Classifier

As the name suggests, the main objective of this block is to classify events and present the output to the operator. The classifier classifies the event as either *'not harmful'* or *'potentially harmful'*. The classifier performs two main functions to classify any event causing distortion. The two functions are analysis of the reported distortions per measuring device and analysis of the reported distortions over the entire set of measuring devices:

a) Reported distortions per device

The first function is to check the number of distortions occurring in each curtailed memory buffer $\widetilde{W}_i$. The value of C_i for each synchronizer block is compared against a threshold th_i. If $C_i > th_i$, a flag is raised, else the classifier doesn't process it further. The value of the threshold is user dependent and is based on the sampling rate of the waveforms. A major parameter for threshold value selection in our case study was comparison between the number of distorted samples recorded during a non-harmful event like switching actions and a harmful event like HIF. The logic behind this is based on observations that a normal switching event might result in a small distortion of signal but the impact will be reflected on one or two samples and it will not repeat itself. Such an event will not exceed the threshold and trigger a warning unnecessarily. However a disturbance leading to a fault or an equipment failure would result in numerous and repeated distortions throughout the waveform, due to which the threshold limit value would be exceeded multiple times and a warning would be triggered.

b) Number of devices reporting distortions

The other function of the classifier block is to check the distortions reported from the waveforms recorded by all the measuring devices in a certain section of the grid. As the input to the classifier has already been synchronized, it is easier for classifier to compare the reported distortions across different devices in the same interval. A relatively stable switching event might not produce distortions in each section of the grid but a fault inducing disturbance would affect the entire grid and would produce distortions in all sections of the grid. The comparison of reported threshold violations over the entire measurement set ensures that false positives are minimized.

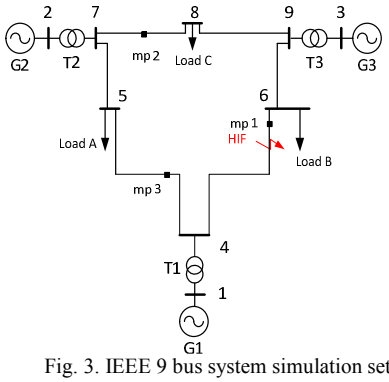

Fig. 3. IEEE 9 bus system simulation setup

III. Simulation Models

A. Choice of Test System

The paper demonstrates the evaluation of the proposed detection method by using standard test systems. The IEEE 9 bus test system [15] is used. The model and its parameters were modelled on RSCAD/RTDS. The model can be seen in Fig. 1. The HIF is simulated for one phase to ground at Bus 6. There are three measurement points (mp), which are mp 1, mp 2 and mp 3. The electrical signals data (current and voltages) are recorded in comtrade format for analysis in MATLAB using the proposed technique. The three measurement points have being chosen few and far between so as to reflect the realistic ground conditions. The placement of measuring points will also help us to evaluate the robustness and effectiveness of the proposed technique as seen in subsequent sections.

B. Choice of HIF Simulation Model

The HIF model is very important because HIF is a very random phenomenon with wide and nonlinear variations in fault current. Specifically designed models would be required in order to accurately recreate HIF in simulation platforms. Simple HIF model with nonlinear impedance has been used in [16], which has been modified further in [17] by including two anti-parallel dc sources with diodes to recreate the asymmetric nature of the HIF current. Hence we use a comprehensive HIF simulation model as proposed in [2].

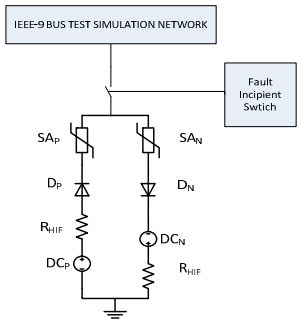

Fig. 4. Comprehensive HIF Simulation Model (RSCAD).

The HIF model is shown in Fig. 4, which was modelled in RSCAD. The model is connected to the IEEE 9 bus test system via means of a fault incipient switch. When the switch is closed it leads to an HIF. The HIF model consists of two DC sources (DC_P and DC_N) in series with ideal resistances (R_{HIF}). The DC resistances are connected to a pair of diodes with opposite conduction in an anti-parallel arrangement (D_P and D_N) respectively. The two diodes are then connected to the nonlinear elements, SA_P and SA_N. These nonlinear element are used to approximate the voltage vs current waveform produced by the HIF phenomenon while DC sources values can be tuned to get the required amount of asymmetry in the fault current.

The behaviour of the HIF is shown in Fig. 5. When the fault inception switch is on, HIF event exhibits two types of behaviours: first is when the positive half cycle of the voltage at Bus 6 (see Fig. 3) is higher than DC_N the current is allowed to flow to the ground and second is when the negative half cycle of the voltage at bus 6 is smaller than the DC_P voltage then the current flow reverses. These

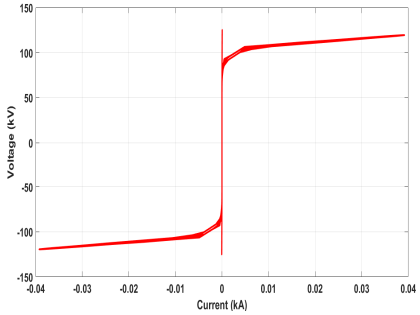

Fig. 5. HIF *v-i* Characteristics

behavioural patterns form the *v-i* characteristics. The characteristics are similar to those obtained from a staged fault in field conditions [18], or a laboratory setup [17].

IV. Simulations and Results

The proposed distortion detection technique is used to detect a single line HIF at Bus 6 in order to inspect its performance versus commercial relay functions.

A. Simulation Setup

A HIL test was conducted on RTDS with Giga-Transceiver Analog Output (GTAO) card transmitting the analog signals from RTDS to an amplifier which recreates the secondary voltage and currents of an ideal voltage and current transformer that are connected at Bus 6. The relay is then connected in the loop next to the amplifier. The settings of the relays were according to the geometrical characteristic of the transmission line. The HIF is simulated at Bus 6 while Distance and Earth directional overcurrent functions were used to protect the bus. The HIL system is depicted in Fig. 6.

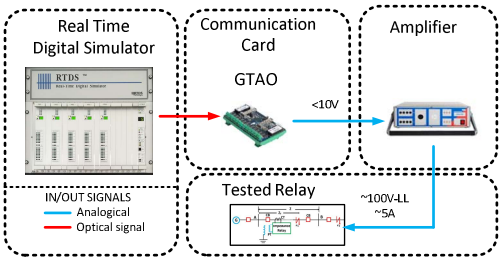

Fig. 6. Configuration of Hardware in the Loop simulation.

1) Distance Protection function

The distance protection test was done with only the distance protection function active. Three zones cover were: zone 1 from 0 to 85% of transmission line (TL), zone 2 from 85% till 150% of the TL, and zone 3 reverse fault. As a validation of the settings first a line to ground fault was simulated, the relay could see the fault without problems. In Fig. 7(a) the impedance trajectory in the quadrilateral protection zones is shown. It can be seen that the fault occurs in zone 1. In Fig. 7(b) the impedance trajectory through time is presented. It can be seen that the impedance decreases considerably indicating a major fault. However, When the HIF is simulated the quadrilateral zones set in the relay are never reached by the impedance trajectory and the relay doesn't record it. The impedance through time for HIF is shown in Fig 8. The change in impedance is less than 4.88%, which indicates an HIF.

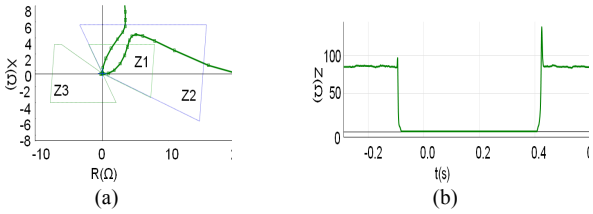

Fig. 7. Impedance trajectory during single line to ground fault: (a) quadrilateral distance characteristic and (b) Impedance through time.

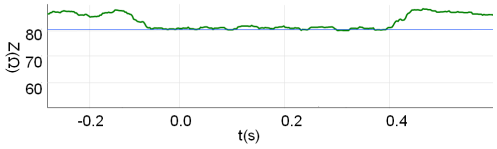

Fig. 8. Impedance through time during a HIF.

2) Directional Protection function

The differential protection test was conducted in the similar simulation setup as the distance protection. The system settings were validated first by conducting a line to ground (LG) fault which was duly detected by the relay. Thereafter, HIF was conducted, which the relay failed to detect. Fig. 9a show relay's current recordings for LG fault. We see a huge increase in current value after the inception of fault whereas in Fig. 9b we see a very small increase in current value (encircled in green). This small increase in current is due to HIF which the relay fails to detect.

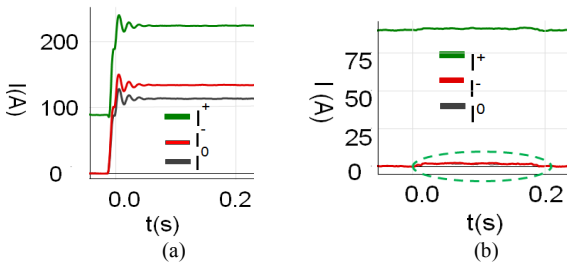

Fig. 9. Directional Relay Current Measurements: (a) Line to Ground Fault and (b) High Impedance Fault

B. Discussion of Results

A snapshot of the current and voltage waveform during the HIF is shown in Fig.10 and Fig.11.

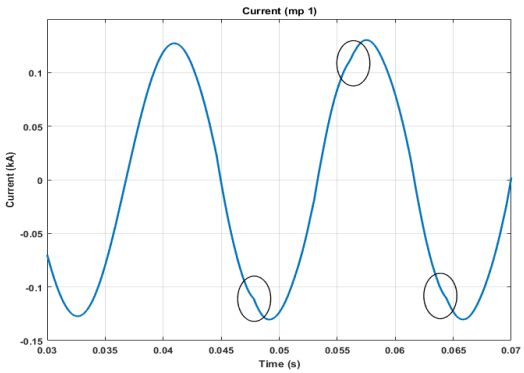

Fig. 10. Current waveform at measurement point 1 (mp 1)

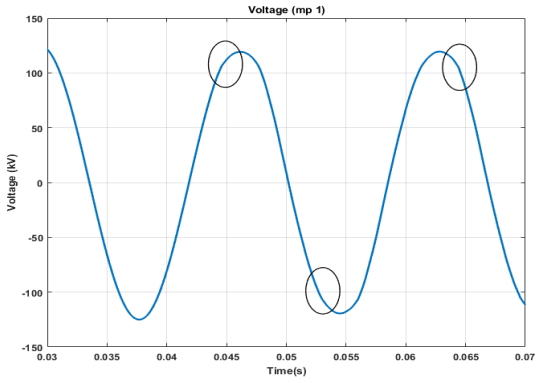

Fig. 11. Voltage waveform at measurement point 1 (mp 1)

Table I
Distortion detection and classification results in the event of High Impedance Fault

Event	Technique Implemented	mp 1 (Number of distortions reported)		mp 2 (Number of distortions reported)		mp 3 (Number of distortions reported)		Common Reportings (Number of distortions)		Classifier
		Voltage Distortions	Current Distortions	Voltage Distortions	Current Distortions	Voltage Distortions	Current Distortions	Voltage Distortions	Current Distortions	
HIF	Distortion Detection Technique	10	12	9	11	7	10	6	9	**Potentially Harmful**
	Commercial Relay: Distance Protection	**NO RELAY TRIP**								
HIF	Distortion Detection Technique	9	12	9	9	7	10	7	9	**Potentially Harmful**
	Commercial Relay: Directional Protection	**NO RELAY TRIP**								

The waveforms are shown for two cycles (one before and one after the inception of HIF). Due to space constraints only the current and voltage measurements from mp 1 are shown. The effect of HIF on magnitude is negligible but there are some distortions in the waveform. The barely visible but not so pronounced distortions have been encircled in black. However, the smallest distortions not clearly visible to the normal eye is easily detected by the Distortion Detection Technique discussed before. A brief summary of results for the three cycles is shown in Table I.

In Table I, we have recorded all the distortions reported (voltage and current) by the Distortion Detection technique for an HIF across different measurement points. Usually the voltage values are more stable hence we see less reported distortions for voltages. The *'common reportings'* column contains the number of common distortions (distortions at the same time) recorded across all the measurement points. This helps to eliminate false reporting's due to inaccuracy or malfunction. The amount of common reporting's also help to assess the extent and severity of the fault. The *'common reportings'* data is processed by the classifier as explained in section III.B.5 to classify an event as either *'not harmful'* or *'potentially harmful'*.

V. Conclusion

The distortion detection technique presented in this paper successfully demonstrates its efficient performance vis-a-vis commercial protective relay in the event of an HIF for different protection schemes. The technique was implemented in a real-time HIL simulation setup to test its effectiveness in as realistic field conditions as possible. Future work will focus on making the technique resilient against noise. Noise can affect the efficiency of detection of distortions. Hence, appropriate noise filters would have to be used to negate the effect of noise.

References

[1] High Impedance Fault Detection Technology, March 1996, Report of PSRC Working Group D15. [Online]. Available: http://www.pes-psrc.org/Reports/High_Impedance_Fault_Detection_Technology.pdf.

[2] S. Gautam and S. M. Brahma, "Detection of High Impedance Fault in Power Distribution Systems Using Mathematical Morphology," in *IEEE Transactions on Power Systems*, vol. 28, no. 2, pp. 1226-1234, May 2013.

[3] M. Sarlak and S. M. Shahrtash, "High-Impedance Faulted Branch Identification Using Magnetic-Field Signature Analysis," in *IEEE Transactions on Power Delivery*, vol. 28, no. 1, pp. 67-74, Jan. 2013.

[4] M. Sedighizadeh "Approaches in high impedance fault detection—A chronological review" Adv. Elect. Comput. Eng. vol. 10 no. 3 pp. 114-12

[5] M. Sarlak S. M. Shahrtash "SVM-based method for high impedance faults detection in distribution networks" Int. J. Comput. Math. Elect. Electron. Eng. vol. 30 no. 2 pp. 431-450 2011.

[6] M. Sarlak and S. M. Shahrtash, "High impedance fault detection using combination of multi-layer perceptron neural networks based on multi-resolution morphological gradient features of current waveform," in *IET Generation, Transmission & Distribution*, vol. 5, no. 5, pp. 588-595, May 2011.

[7] S. R. Samantaray, B. K. Panigrahi and P. K. Dash, "High impedance fault detection in power distribution networks using time-frequency transform and probabilistic neural network," in *IET Generation, Transmission & Distribution*, vol. 2, no. 2, pp. 261-270, March 2008.

[8] A. H. Etemadi M. Sanaye-Pasand "High impedance fault detection using multi-resolution signal decomposition and adaptive neural fuzzy inference system" Inst. Eng. Technol. Gen. Transm. Distrib. vol. 2 no. 1 pp. 110-118 2008.

[9] M. Michalik M. Lukowicz W. Rabizant S. J. Lee S. H. Kang "New ANN-based algorithms for detecting HIFs in multigrounded MV networks" IEEE Trans. Power Del. vol. 23 no. 1 pp. 58-66 Jan. 2008.

[10] A. R. Sedighi M. R. Haghifam O. P. Malik M. H. Ghassemian "High impedance fault detection based on wavelet transform and statistical pattern recognition" IEEE Trans. Power Del. vol. 20 no. 4 pp. 2414-2421 Oct. 2005.

[11] A. Girgis "Analysis of high-impedance fault generated signals using a Kalman filtering approach" IEEE Trans. Power Del. vol. 5 no. 4 pp. 1714-1724 Oct. 1990.

[12] S. R. Samantaray P. K. Dash "High impedance fault detection in distribution feeders using extended Kalman filter and support vector machine" Eur. Trans. Elect. Power 2009

[13] R. Bhandia, M. Cvetkovic and P. Palensky, " Improved Grid Reliability by Robust Distortion Detection and Classification Algorithm," *2018 IEEE PES Innovative Smart Grid Technologies Conference Europe (ISGT-Europe)*, in press.

[14] Yong Cheol Kang, Ui Jai Lim, Sang Hee Kang and P. A. Crossley, "Compensation of the distortion in the secondary current caused by saturation and remanence in a CT," in *IEEE Transactions on Power Delivery*, vol. 19, no. 4, pp. 1642-1649, Oct. 2004.

[15] The Illinois Center for a Smarter Electric Grid (ICSEG), "WSCC 9-Bus System," *Power Cases*, [Accessed. April 1, 2018]. [Online]

[16] D. Yu S. Khan "An adaptive high and low impedance fault detection method" IEEE Trans. Power Del. vol. 9 no. 4 pp. 1812-1821 Oct. 1994.

[17] A. Emanuel "High impedance fault arcing on sandy soil in 15 kv distribution feeders: contributions to the evaluation of the low frequency spectrum" *IEEE Trans. Power Del.* vol. 5 no. 2 pp. 676-686 Apr. 1990.

[18] A. Sultan "Detecting arcing downed-wires using fault current flicker and half-cycle asymmetry" IEEE Trans. Power Del. vol. 9 no. 1 pp. 461-470 Jan. 1994.